Meteorology triggering factors analysis for rainfall induced hydrogeological events in alpine region

Andrea Abbate[1], Monica Papini[1], Laura Longoni[1]

[1] Department of Civil Engineering (DICA), Politecnico di Milano, Milano 20133, Italy

5 *Correspondence to*: Laura Longoni (laura.longoni@polimi.it)

Abstract. This paper presents an extended back analysis of the major hydrogeological events that occurred in the last 70 years in the alpine area of the Lombardy region, Italy. This work is focused on the description and the interpretation of the major meteorological triggering factors that have caused these mass movements.

The triggering factors for each hydrogeological event were analysed into twofold approaches, with the final intent of ranking

10 their magnitude in terms of consequent damages. Firstly, an analysis of precipitation was conducted using local rain-gauge data, comparing them against rainfall-threshold curves proposed by several authors. Moreover, the return time of precipitation and the information about the spatial extension of the triggering factors were considered for the assessment of an empirical magnitude index of the hydrogeological event. Secondly, considering the currently available meteorological reanalysis database, provided globally by National Centres of Environmental Prediction (NCEP), additional information on

15 the dynamics, the nature and intensity of meteorological triggers were taken into account. The two approaches were compared throughout two indexes that tried to assess the strength of rainfall phenomena: the first one is empirical while the second one is physical.

The results obtained from the application of the two methodologies have been discussed. The rainfall method permits to highlight which are the critical hydrogeological events, not giving any quantitative information about their magnitude. The

20 second approach analyses better the characteristic and the dynamic of meteorological triggers, suggesting, through a physical index, a quantitative ranking of their intensities that has revealed to be a good predictor for the magnitude of hydrogeological rainfall-induced events.

1 Introduction

Landslides represent one of the main hydrogeological hazards in Alpine and Apennines regions (Albano et al., 2017; Ballio

25 et al., 2010; Caine, 1980; Gao et al., 2018). Italy is a country historically affected by a diffuse hydrogeological fragility of the environment (Longoni et al., 2016) and mountain slopes are the most vulnerable places where landslides and flash floods can occur (Iverson, 2000; Longoni et al., 2011; Montrasio, 2000; Montrasio and Valentino, 2016). This is the case of Valtellina (Lombardy) in 1987 as well as Piedmont in 1994 and 2000 and Genova city in 2011 and 2013, which were affected by several flash floods and landslides phenomena. All of these catastrophic events have been caused by exceptional

30   meteorological events that rarely occur and have particular features regards their duration and their intensity (Ceriani et al., 1994).

In the context of hydrogeological risk prevention, urban planners and infrastructure engineers have to deal with the analysis of triggering factors and need instruments for its quantification (Ozturk et al., 2015; Papini et al., 2017; Piciullo et al., 2017; Rossi et al., 2019). In this paper, a back analysis of the meteorological triggers of past hydrogeological events is presented.

35   Indeed, a quantitative study of local precipitation is mandatory to correlate these meteorological events with landslide failures (Corominas et al., 2014; Guzzetti et al., 2007).

A common approach used consists of the analysis of the return period (RP) of the triggering rainfall (Caine, 1980; Iverson, 2000). It is not trivial to evaluate the recurrence of a flood or a landslide unless we make a hypothesis of iso-frequency with the RP of precipitation (De Michele et al., 2005; ISPRA, 2018). For a flood that occurred in a flood plain or in a large valley,

40   this hypothesis is generally acceptable due to the fact that it can happen even though a large amount of water is available, coming from an intense and prolonged meteorological event (Albano et al., 2017; De Michele et al., 2005). For a landslide failure, defining a return period is not a common practice because it is not a periodic event but a sudden collapse (ISPRA, 2018). This is particularly true for complex and deep landslide where the triggering factors are intimately bounded with the local predisposing factors, i.e. the territory morphology, geology, etc. (Ciccarese et al., 2020; Guzzetti et al., 2007; ISPRA,

45   2014, 2018; Longoni et al., 2016; Montrasio, 2000; Ozturk et al., 2015; Papini et al., 2017). Therefore, try to interpret this cause-effect relationship looking only at the rainfall series cannot be used.

However, for shallow landslides and debris flows hazard assessment, are considered the rainfall intensity-duration curves (Ceriani et al., 1994; Ciccarese et al., 2020; Gao et al., 2018; Longoni et al., 2011; Olivares et al., 2014; Rappelli, 2008; Rosi et al., 2016; Rossi et al., 2019). These define a rainfall threshold for a specific region on which, taking into account the

50   duration and the average intensity of the rainfall episode, a landslide could be triggered. This interpretation is acceptable, considering this type of landslide rainfall-induced (Ceriani et al., 1994; Guzzetti et al., 2007; Piciullo et al., 2017; Rosi et al., 2016). These thresholds data are calibrated looking at the past events occurred in the area and directly correlated with the nearest rain gauge measures (Rappelli, 2008). Intrinsically they include the susceptibility of the local territory to landslide failure so their usability generally can't be extended to other regions (Caine, 1980; Guzzetti et al., 2007; ISPRA, 2018;

55   Longoni et al., 2011). On the other hand, this method is widely used for predicting the occurrence of shallow landslide and debris flow events but, due to its empirical nature, it is rather approximate and leads sometimes to "false alarm" detecting (Abbate et al., 2019; Guzzetti et al., 2007; Peres et al., 2018).

Even though the rainfall return period estimation and rainfall thresholds have been widely used in different parts of the world (Gao et al., 2018), some open questions still exist. Are these approaches sufficient for a complete description of triggering

60   factors? Can rainfall analysis be improved considering also other meteorological variables, which could better describe the rainfall events and the linked consequences?

Generally, a local study on the triggering causes is not completely descriptive of the real magnitude of the meteorological triggering event (COPERNICUS, 2020; Rotunno and Houze, 2007; Stull, 2017). This is particularly true in mountain areas

where the territory enhances the heterogeneity of rainfall field that is not able to exhaustively represented only taking into account the local rain gauge network (Rotunno and Houze, 2007). In particular, the type of rainfall events cannot always be recognized directly from rain gauge time-series so that other meteorological variables should be taken into account for its description. This is crucial because different precipitation type can affect the characteristics of the hydrogeological failures (Corominas et al., 2014; Guzzetti et al., 2007). An intense but rather localized rainfall, such as a thunderstorm, could trigger a certain type of hydrogeological issues, such as shallow landslides and soils slips (Montrasio, 2000). On the other hand, a persistent orographic rainfall, which could affect an entire region for several days, may have completely different effects on the territory, enhancing its hydrogeological fragility (Longoni et al., 2011; Rotunno and Houze, 2007; Tropeano, 1997). Therefore, a more complete description of the type of triggering factor is necessary to better explain the territorial hydrogeological dynamics.

The goal of this paper is to investigate the relationship between hydrogeological issues and their triggering factors in a broader sense, starting from the back analysis of past hydrogeological events, where landslide and flash flood occurred. The alpine region in the northern part of Lombardy, Italy, was considered because of its past critical hydrogeological events (CNR, 2020; ISPRA, 2014; Rappelli, 2008; Tropeano, 1997). Triggering factors were analysed into twofold approaches. The first one uses only local rainfall data applying the threshold curves method as a reference for detecting shallow landslide failure. The second considers also meteorological reanalysis maps provided globally by National Centres of Environmental Prediction (NCEP) (Kalnay et al., 1996; MeteoCiel, 2020; NOAA, 2020) where is possible to gather additional information about the spatial and temporal evolution of the triggering events at larger scale (Andrews, 2010; Grazzini, 2007; Grazzini and Vitart, 2015; Stull, 2017).

The paper will be organized as follows: in section 2 is presented the databases of the historical hydrological events and the materials and methods adopted in our analysis of triggering factors related to these events. In section 3 the results and relative discussion are reported, with some comparisons and comments regarding the two approaches and in section 4 some final remarks and conclusions of the ongoing research work are reported.

2 Data, Methods and Models

This section presents the methodology followed for the back analysis.

2.1 Historical database of hydrogeological events

A group of past hydrogeological events has been considered for the alpine area of Sondrio Province, northern Lombardy, Italy, Figure 1. This area was affected by exceptional hydrogeological events in July 1987 causing extended damages and loss of lives (CNR, 2020). The most important and severe was the Val Pola landslide that occurred in the upper part of Valtellina and happened as a sudden collapse of 40 million cubic meter of old debris, destroying 5 villages and six hamlets with 35 people died of various disaster-related causes (Tropeano, 1997). On the other hand, the entire province was also

95 affected mainly by diffuse hydrogeological episodes such as shallow landslide and flash floods, that caused people injuries and comparable damages to infrastructure and buildings, estimated in 2 billion of euros. These hydrogeological issues were caused by a rather intense and prolonged rainfall episode (Rappelli, 2008; Tropeano, 1997) and the effects were enhanced by rapid glacier melting increased by high-altitude summer temperatures.
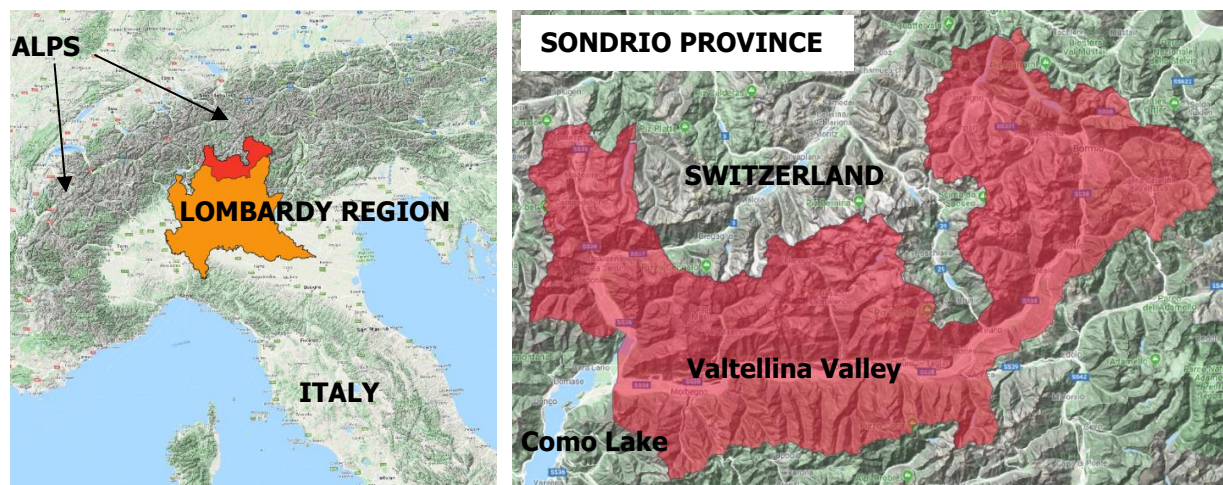
Figure 1: Case Study Area of Sondrio province, northern Lombardy, base-layer from © Google Maps 2020.

100 The back analysis has considered also other critical hydrogeological episodes like the 1987 that affected the Sondrio Province. Two different data sources have been used to collect data for the analysis of the historical hydrogeological events: the "Aree Vulnerate Italiane" (AVI) database and the "Inventario Fenomeni Franosi Italiano" (IFFI) database (CNR, 2020; ISPRA, 2014). The AVI database is directly available inside a geoportal-web site that is managed by CNR (Centro

105 Nazionale della Ricerca) and the IFFI database, available from the national geoportal website (CNR, 2020; ISPRA, 2014). The data stored collects historical information from past natural disaster starting from the medieval age up to nowadays. Looking at the available time-series, data are not homogeneous and the lack of information is generally diffused (CNR, 2020; ISPRA, 2018). For the area of Sondrio Province, a quite extensive historical bibliography was found in literature (Ceriani et al., 1994) that considers all the events starting from 1850 up to 2000. In this case, the two databases' consistency was evaluated, and redundant records have been corrected. Then, a merging operation between the AVI and the IFFI

110 database information was needed for the years comprised between 2000 and 2019.

The period chosen for the back analysis is comprised between 1951 and 2019. Indeed, systematic monitoring of the precipitation and temperature started in Italy since 1951 by SIMN (Servizio Idrografico e Mareografico Nazionale) and looking at the antecedent periods these data were missed or characterized by several uncertainties or errors (ISPRA, 2019).

115 The available rain gauge data series were gathered from local archives of SIMN (ISPRA, 2019) and ARPA Lombardia (Agenzia Nazionale per la Protezione dell'Ambiente) (ARPA Lombardia, 2020). These series have been conventionally recorded on daily bases until the 2000s years so "a daily rain" represents the maximum resolution of our dataset before that

period. Starting from 2001, the increased temporal resolution available that moved to a sub-hourly time-step increased the accuracy of the rainfall analysis.

120 The list of the hydrogeological events analysed in the study and their description retrieved from AVI and IFFI databases is reported in Table 1.

Table 1: Hydrogeological events recorded from 1951 up to 2019 considered for the back-analysis study. In the table are reported the starting and ending date for each event, the typology of the meteorological triggers, the hydrogeological effects on the territory, the information about the extension of the territorial area affected [km^2], the extreme localized events (EXL) and the more diffuse
125 **ones (DIF), the cumulated rain [mm] gathered by local rain gauges and the event duration [days].**

YEAR	START	FINISH	METEO TYPE	EFFECTS	EXTENSION TYPE	ESTIMATED AFFECTED AREA [km^2]	CUMULATED RAIN [mm]	EVENT DURATION [days]
1951	7 august	8 august	Heavy rainfall	Flash Floods	EXL	500	218	2.0
1953	17 july	18 july	Heavy rainfall	Flash Floods	EXL	125	83.8	1.0
1960	15 september	17 september	Heavy rainfalls	Landslide and Floods	DIF	2000	115.6	2.0
1966	3 november	5 november	Prolonged rainfalls	Landslides and Floods	DIF	3000	128.6	3.0
1983	21 may	23 may	Heavy rainfalls	Landslides	EXL	100	208.6	3.0
1987	16 july	19 july	Prolonged rainfalls	Landslides and Floods	DIF	4000	254.8	3.0
1997	26 june	29 june	Prolonged rainfalls	Landslides and Floods	EXL	200	275	3.0
2000	13 november	17 november	Prolonged rainfalls	Landslides	DIF	2000	218.7	4.0
2002	13 november	18 november	Prolonged rainfalls	Landslides	DIF	3000	308.8	5.0
2008	12 july	13 july	Heavy rainfalls	Landslides	EXL	240	60	0.5
2018	27 october	30 october	Prolonged rainfalls	Landslides	DIF	3000	242.4	3.6
2019	11 june	12 june	Heavy rainfall	Landslides and Floods	EXL	700	150	0.7

The precise location of each hydrogeological event was not directly reported in the dataset, but an indication of the municipalities affected by hydrogeological issues was present. These data were taken into consideration for defining the extension of the triggering phenomena and were corrected looking at the recorded rain gauges series. In particular, rainfall

130 events were distinguished in two types: extremely localized events (EXL), with an influence area lower than 1000 km^2, or diffuse events (DIF), with significant territorial diffusion greater than 1000 km^2. This value has been motivated considering the nature of the meteorological triggers: "EXL" were generally associated with convective rainfall phenomena which extension has an order of 10 x 10 km^2 and "DIF" were characterized by diffuse and uniform rainfall with an extension around 100 x100 km^2 (Martin, 2006; Rotunno and Houze, 2007).

135 The dataset analysis of Table 1 shows a clear seasonal distribution of the events mainly concentrated during summer and autumn. July and November are the months much more prone to hydrogeological events and this strong seasonality highlights that triggers phenomena involved may have a different nature (Martin, 2006; Rotunno and Houze, 2007). In July,

meteorological events are characterized mainly by high intensity and short duration with a typical convective behaviour of precipitation (thunderstorms), and their average duration is generally around 1 or 2 days. In particular, 1951, 1953, 1987 and
140   2008 events happened during the summer season and rainfall cumulated were comprised between 100-200 mm, apart from 1987 and 1997 that were rather exceptional (254 mm and 275 mm in three days). During October and November, rainfall events are characterized by higher persistency (4-5 days) and rainfall cumulated can easily reach amounts around 250-350 mm, such as for the events that happened in 2000, 2002 and 2018. They are usually associated with extratropical cyclone structures that moving eastward from Atlantic Ocean can affect directly the Alpine mountain range (Martin, 2006).
145   These observations from the dataset have been studied in deep from a quantitative viewpoint considering the two approaches proposed: the traditional rainfall approach and the meteorological reanalysis approach.

2.2 Traditional Approach: Rainfall Threshold Curves and Rainfall Return Period analysis

The rainfall data were elaborated considering the spatial extension of the triggering events, i.e. rainfall field characteristics. For the "EXL" data, the nearest rain gauge or at least the 2 nearest rain gauges were chosen as local rainfall data. For the
150   "DIF" group, all the available daily rain data RR_i in the affected territory have been considered and averaged with respect to the number of rain gauges stations "n" in order to obtain a representative value for RR.

$$RR = \frac{\sum_{i=1}^{n} RRi}{n} \tag{1}$$

Then, the average daily rainfall rate RR was calculated dividing the cumulative rainfall by the duration D. The results were then plotted against the local rainfall intensity-duration threshold curve. For the examined area was considered a group of threshold curves proposed in the literature by several authors.
155   The "Caine" curve (Caine, 1980) is the general one, valid for shallow hydrogeological processes around the world, Eq. (2.a). The "Ceriani" curve (Ceriani et al., 1994) was proposed in 1994 and was calibrated directly on the recorded data available in Sondrio Province, Eq. (2.b). A more recent study conducted by (Guzzetti et al., 2007) has proposed a new set of rainfall threshold curves valid for central and southern Europe, considering a distinction among different climate types. In our study, three of them have been selected: the general one Eq. (2.c), the curve valid for mid-climate Eq. (2.d) and the one suitable for
160   highlands Eq. (2.e). All the rainfall threshold curves have a monomial expression where the D is the duration of the rainfall [hours], and the I is the average rainfall intensity [mm/h].

$$I = 14.84 \, D^{-0.39} \tag{2.a}$$

$$I = 20.01 \, D^{-0.55} \tag{2.b}$$

$$I = 8.67 \, D^{-0.61} \tag{2.c}$$

$$I = 18.6 \, D^{-0.81} \tag{2.d}$$

$$I = 8.53 \, D^{-0.64} \tag{2.e}$$

A further step on rainfall analysis dealt with the evaluation of the correspondent return period (RP). The RP is directly associated with the intensity of the rainfall because it expresses the probability of recurrence of a particular rainfall event on

a location (Corominas et al., 2014; De Michele et al., 2005). Using the Curve of Pluviometric Possibility (CPP) (De Michele
165   et al., 2005) available for the Lombardy region and provided by (ARPA Lombardia, 2020), the RP of precipitation was
estimated for each event. Localized events "EXL" were treated separately with respect to the diffuse "DIF" ones. For the
localized events, the on-site coefficient of CPPs has been used but for the diffusive ones, a spatially averaged value of the
coefficients has been elaborated for the area of interest.

2.3 Reanalysis Approach: NCEP Reanalysis Maps

170   To improve the analysis of triggering factors, the database was studied considering other variables associated with the
meteorological event. In particular, the National Centre for Environmental Prediction (NCEP) data (Kalnay et al., 1996;
MeteoCiel, 2020) were examined. The NCEP reanalysis maps are a valuable instrument for investigating the past evolution
of meteorology around a target area (Faggian, 2015; Grazzini, 2007; Rotunno and Houze, 2007; Stull, 2017). They have a
spatial resolution of 2.5° x 2.5° degrees of latitude and longitude, covering the whole planet with a temporal frequency of 12
175   h. These maps contain information about temperature and pressure distribution at different geopotential heights, i.e. 850 hPa
and 500 hPa, to describe air mass advection and front formations. The pressure values reported at sea level are valid
indicators of a cyclone or anticyclone structure developments at regional scale (Andrews, 2010; Grazzini and Vitart, 2015;
Stull, 2017). Moreover, the wind fluxes velocities are important for establishing the spatial and temporal evolution of a
particular rainfall event (Andrews, 2010; Grazzini, 2007; Stull, 2017).

180
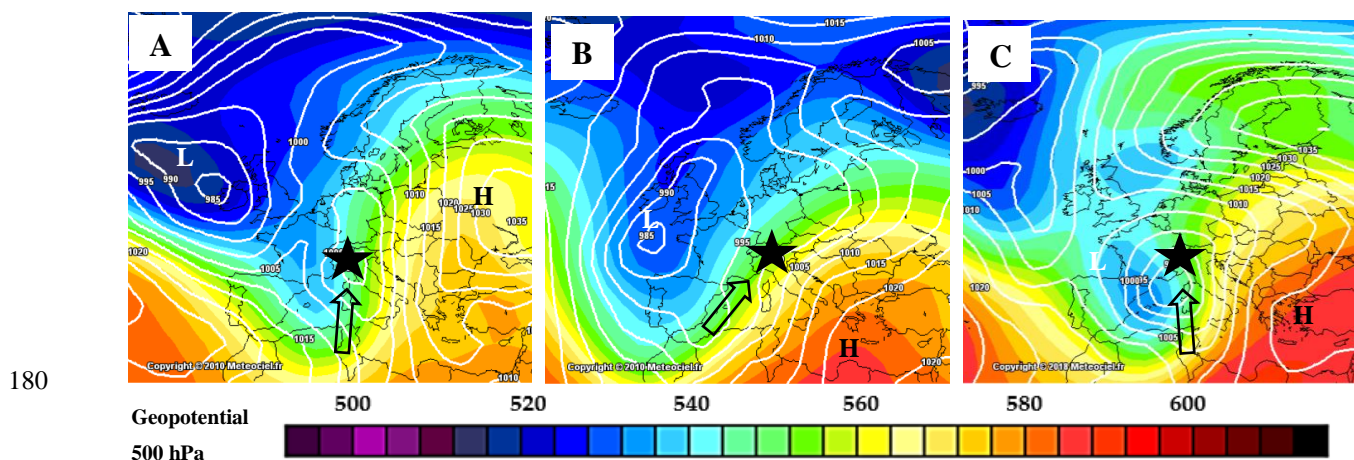
Figure 2: Reanalysis maps from NCEP reporting the Sea-Level Pressure and 500 hPa Pressure (colours) for 1966 (A), 2002 (B) and 2018 (C) events where the black star is the Sondrio Province position, adapted from (MeteoCiel, 2020), modified after.

185   A qualitative looking at the reanalysis maps for each considered event highlights some similarities regarding the
meteorological configuration of air masses. Not surprisingly, the major hydrogeological events have occurred during strong
extratropical cyclone (EC), as described in Figure 2.

ECs are important meteorological phenomena that develop in the Atlantic Ocean near the British Islands and are moved eastward through the Mediterranean area thanks to the dynamic of the Rossby waves at planetary scale (Grazzini and Vitart, 2015; Martin, 2006). These generate at the boundary of the polar vortex strong jet streams that can move air masses in the direction of the southern Alps, as is represented in Figure 2. Across the southern flank of Alps, one of the critical consequences of this configuration is the enhancement of persistent and heavy orographic precipitation (Rotunno and Houze, 2007) thanks to the instauration of a strong southern moist and warm flow, the "Scirocco" wind, as reported by (Grazzini, 2007). Rainfall intensities can reach remarkably high amounts if these conditions are prolonged for several days, leading up to 400 mm in 2/3 days (Grazzini, 2007; Rotunno and Houze, 2007). In addition, the presence of convection especially during the summer season may add another level of complexity, producing a further enhancing of local rainfall rates (De Michele et al., 2005; Rotunno and Houze, 2007).

This dynamic is characterized by some peculiarities that are necessary to be understood for interpreting the local scale rainfall effects on the territory. Therefore, using the NCEP maps, a synthetic model proposed by (Godson, 1948; Martin, 2006; Stull, 2017) was chosen for the estimation of a strength index related to the extratropical cyclone intensity. The model calculates indirectly the Sea-Level Pressure Tendency (SLPT), the time-variation ratio of sea-level atmospheric pressure $\Delta p_{sl}/\Delta t$ [hPa/h], that represents an indicator of the strength of a cyclone structure (Andrews, 2010; Godson, 1948; Martin, 2006; Stull, 2017; Wallace and Hobbs, 2006). In general, this ratio is higher, in an absolute sense, when the EC is more intense. According to (Stull, 2017), this index is obtained as a sum of three different influencing factors that correspond to the most important processes implicated in the dynamic evolution of extratropical cyclone:

$$\frac{\Delta p_{sl}}{\Delta t} = T_1 + T_2 + T_3 \qquad (4)$$

- T_1 expresses the "upper-level air divergence" due to jet streams, which remove air mass from an ideal atmosphere air column. W_{MID} [m/s] is the mean air column vertical velocity, evaluated considering the continuity equation in the proximity of the local change of jet stream velocity gradient. $\rho_{MID} = 0.5 \; kg/m^3$ is the average density of air column and $g = 9.8 \; [m/s^2]$.

$$T_1 = -g \, \rho_{MID} \, W_{MID} \qquad (4.a)$$

- T_2 is the "atmosphere boundary layer pumping", that causes the horizontal wind to spiral inward toward a low-pressure center. The air density of the boundary layer is $\rho_{BL} = 1.112 \; kg/m^3$, $g = 9.8 \; [m/s^2]$ and W_{BL} is the vertical velocities at boundary-layer calculated using the approximation proposed by (Stull, 2017) for cyclone structures.

$$T_2 = g \, \rho_{BL} \, W_{BL} \qquad (4.b)$$

- T_3 is the "latent heating" due to water vapor condensation in rainfall. It comes from the theory of thermodynamic transformations of water vapor in the atmosphere where all the parameters for rain condensation processes are stored in the term $b = 0.082 \; [kPa/mm]$ and RR [mm/h] is the average hourly rainfall rate. In the model proposed, the information related to the local rainfall intensity is considered only in

220   this term while the other is in the function of the meteorological parameters retrieved from NCEP reanalysis maps [27].

$$T_3 = -b\, RR \qquad\qquad (4.c)$$

When the balance in Eq. (4) is negative the cyclogenesis occurs. Indeed, the term T1 and T3 have a negative contribution and during the cyclone formation (cyclogenesis) participate in the decreasing of the SLPT index. Figure 3 reports how the model works, considering the contribution of each four components across the timeline (A to G) during the phase of EC formation (i.e. cyclogenesis, from A to D) and EC dissolution (i.e. cyclolysis, form D to G). When the balance in Eq. (4) is

225   negative the cyclogenesis occurs so that the critical phase of the EC is in the proximity of point D where negative terms overcome the positive one.
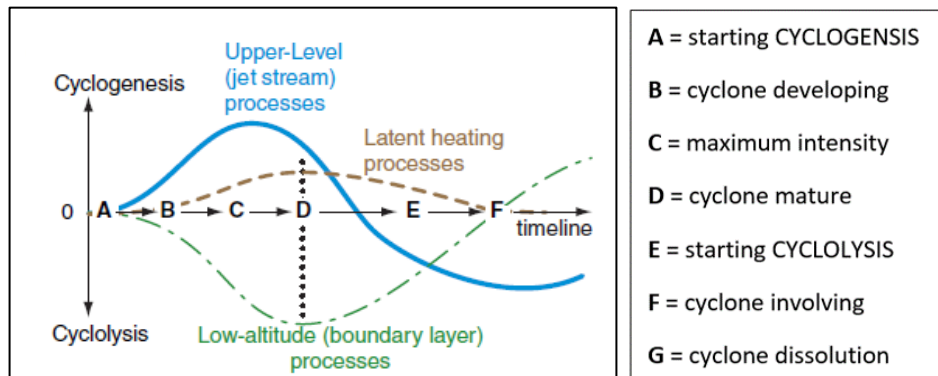
Figure 3: Qualitative temporal evolution of each of four terms T1, T2 and T3 during cyclone phases (A to G) and their contribution to cyclone formation (cyclogenesis) and cyclone dissolution (cyclolysis), proposed in (Stull, 2017), modified after.

230   **3 Results and Discussion**

The first approach, based on the definition of critical events against threshold curves, carried out the analysis only on rainfall parameters, i.e. the rain intensity (I) and the duration (D). The second extended the precipitation study considering also other meteorological parameters, reported inside NCEP reanalysis maps, and applying the model proposed in Eq. (4) for EC intensity.

3.1 Approach 1: the Rainfall Analysis

235

Considering the average daily rain rate *I* and the duration *D* of the rainfall episodes reported in Table 1, these data were plotted against the rainfall threshold curves listed from Eq. (2.a) to Eq. (2.e) inside Figure 4. A large number of events can be clustered in the right-bottom corner of the graph due to their characteristics of a rather long duration 2-4 days and slightly low intensities. Only the event of 2019, 2008 and 1953 are dispersed on the other side of the graph where the duration is

240 around or less than a day.

Considering the thresholds proposed by (Guzzetti et al., 2007), all the events points are correctly settled above lines. In particular, no big differences are seen among the general one (3), the curve valid for mid-latitude climate (4) and the one valid for highlands climate (5). On the other hand, the thresholds proposed by Ceriani (2) and Caine (1) are settled above the previous. The "Ceriani" one seems to fit very well the data, posing only the 1966 event slightly below the curve and the

245 1953 and 1960 close to the curve. This result was expected because the "Ceriani" threshold has been calibrated using a dataset of local events until 1994. Conversely, the "Caine" threshold seems to work worst rather than the previous. 1953, 1960 and the 1966 events are not identified as critical and appear below the curve. In this case, the threshold curve has been unable to detect these events. Moreover, the 1997 and 2000 are settled borderline on the curve.
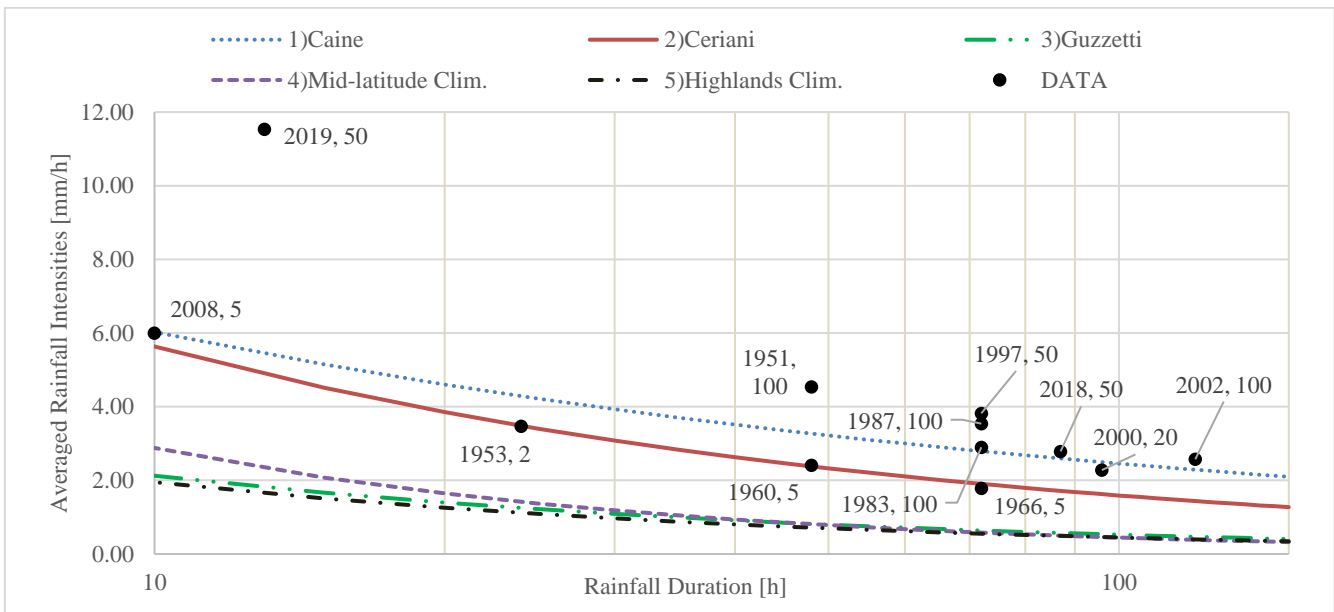
250 **Figure 4: Intensity-Duration relationship for considered events and relative precipitation RP.**

For each critical event, the related rainfall return period has been also specified in Figure 4. According to (Gao et al., 2018; Iida, 2004; Rosso et al., 2006), a beam of rainfall intensity-duration curves can be elaborated including their dependence from RP. Considering the "Ceriani" threshold, the critical events that exhibit higher RPs are located at higher distances from the curve and, on the other hand, the events with a small return time are settled nearer. Therefore, the vertical distance

255 between the curve and the critical event point could be addressed as a possible indicator of the magnitude of the

hydrogeological events, but the empirical correlation founded in these literature analyses suggests that it may be subjected to large uncertainties (Gao et al., 2018).

In conclusion, the threshold curves assess if a rainfall event can trigger hydrogeological issue, but no further detailed information can be retrieved to the effective magnitude of the event occurred. The physical nature description of the rainfall

260 phenomena is generally missed and a relative comparison among the different critical events cannot be properly done. In addition, the wide range of threshold curves available for the area and their empirical evaluation increase the uncertainty around the assessment of the critical events. Moreover, the small database of our study does not permit us to clearly assess a magnitude of the hydrogeological event simply looking at these distances among the threshold and each critical event point.

A further step of the analysis has been carried out considering not only the information about the intensities of the triggering

265 phenomena but also their spatial extension, i.e. "EXL" or "DIF".
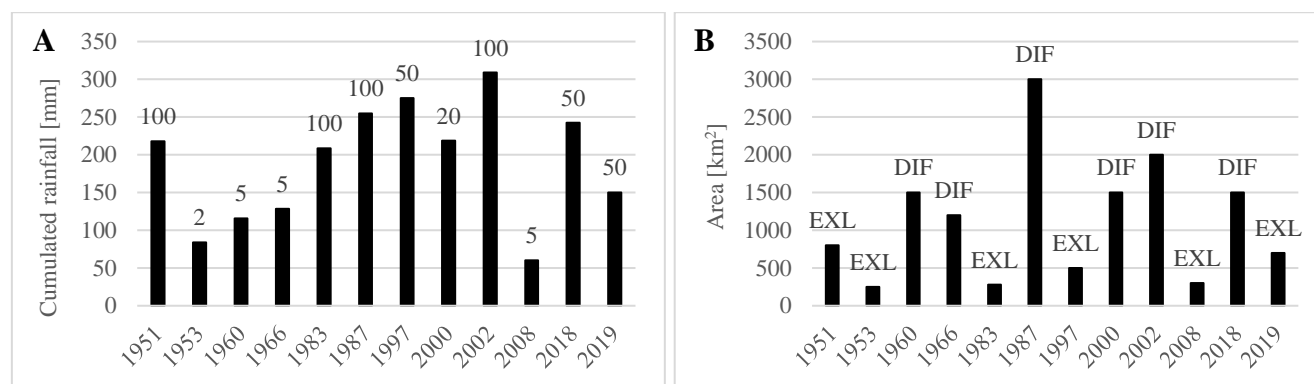
Figure 5: Cumulated rainfall and RP of triggering events (A) and the Area affected by hydrogeological issues (B).

Looking at Figure 5.A, the Sondrio Province has experienced at least four exceptional rainfall events with a return period equal to 100 years: 1951, 1983, 1987 and 2002. From RP analysis, they were ranked with the same intensity but among them

270 1987 has been recorded historically as the most catastrophic one, i.e. with the highest magnitude, that affected the area in the second half of the XX century. This apparent contradiction has a possible explanation considering the information about the spatial extension of the affected areas, as reported in Figure 5.B, which is a property strictly related to the nature of the rainfall event (Corominas et al., 2014; Gao et al., 2018). Those were not directly considered in RP evaluation that takes into account only the local amount of precipitation or an averaged value across a region. Therefore, if only the RP is considered,

275 1983 is intended to be intense as 1987, but, considering the spatial distribution the 1983 event affected only a limited area and the 1987 spread across the entire province. In this light, the RP information leads to a false interpretation of the nature of the two triggering phenomena and it cannot be considered directly for establishing a magnitude of the related hydrogeological consequences on the territory.

According to (Corominas et al., 2014), the hazard intensity of a hydrogeological event can be addressed considering three

280 different contributes. Excluding the territorial susceptibility, the extension of the affected area and the intensity of the triggers are the other two main components. In scientific literature, it does not exist a unique method for the magnitude

assessment of a hydrogeological episode because its quantification depends on the type of triggered phenomena involved and on the scope of the hazard study (Corominas et al., 2014; ISPRA, 2018). In the special case of the rainfall-induced shallow landslides, a logarithmic function seems to explain roughly the relationship among the event magnitude and the

285 characteristics of the trigger. According to (Malamud et al., 2004), a magnitude index can be defined as a logarithmic function of the number of triggered landslide and considering the study of (Bovolo and Bathurst, 2011; Frattini et al., 2009; Reid and Page, 2003), a similar frequency-magnitude relation can be found for the intensity of rainfall event. Based on these evidences, two indices m_1 and m_2 have been considered for defining the magnitude of analysed hydrogeological events, taking into account the fact that both the spatial extension and the intensity of triggering are involved in its definition.

$$m_1 = \log_{10}(Area\ Affected) \tag{5.a}$$

$$m_2 = \log_{10}(Return\ Period) \tag{5.b}$$

290 These two indexes were calculated and normalized among 0 and 1 for each considered event and then compared. Not surprisingly, looking at Figure 6, they brought complementary information. In the case of 1987 and 2002, both events experienced higher values of the index m_1 and m_2 that are in accordance with the previous observations, i.e. intense event and rather spatial diffuse. On the contrary, 1983 shows a low value of m_1 and high one for m_2, i.e. a very localized event but also particularly intense. In order to give a unique and quantitative ranking of the event's magnitude, for each events the

295 indices m_1 and m_2 have been averaged (AVG). The latter was considered as a reference for the comparison with the SLPT physically based index proposed in the meteorological reanalysis approach.
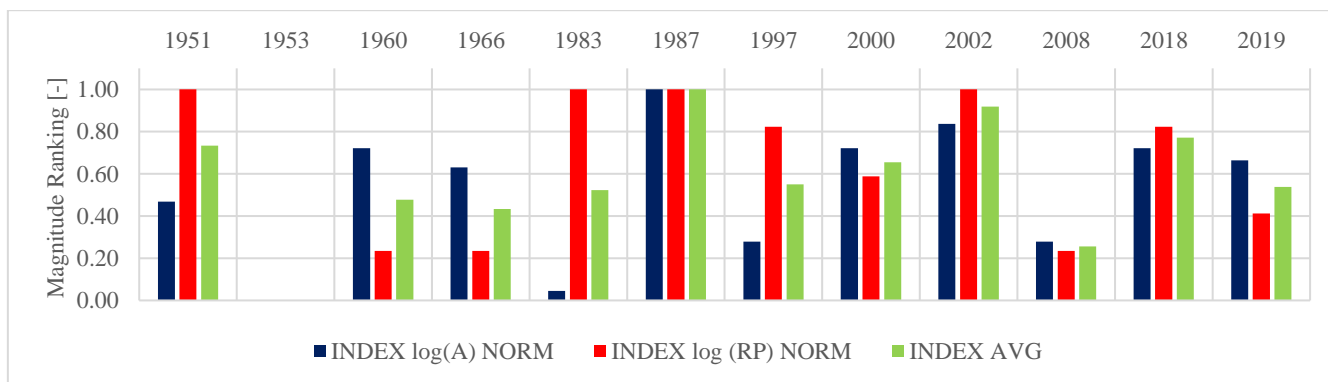
Figure 6: Event magnitude ranking considering the two normalized index "log(A)" and "log(RP)" and their average "AVG".

3.2 Approach 2: Meteorological Analysis

300 The second approach consists of the application of the model proposed by (Stull, 2017) and described in Eq.(4). Atmospheric pressure gradients, wind velocities, and air masses advection through the Alpine region were studied for feeding each of the model components illustrated in the Equation (4.a), (4.b), and (4.c). According to (Stull, 2017), the sea-level pressure tendency index (SLPT) $\Delta p_{sl}/\Delta t$ [hPa/h] was calculated for assessing the intensity of the meteorological

triggering events. This estimation has been done in correspondence to the critical phase of each event, i.e. the "D" phase of
305 the scheme reported in Figure 3.

3.2.1 Wind Components

For determining the $T1$ term ("upper layer divergence" Equation (4.a)), the dynamic of geostrophic wind components was
examined considering the NCEP reanalysis maps.

Geostrophic wind is the theoretical wind that would result from an exact balance between the Coriolis force and the pressure
310 gradient force and it is a valuable first approximation of the general circulation of the air masses at a regional scale
(Andrews, 2010; Martin, 2006; Stull, 2017). Generally, intense geostrophic wind means that the pressure gradient between a
low and high pressure is sharp, and it is associated with strong EC structures (Figure 2). Therefore, geostrophic wind
velocity is an indicator of the meteorological event intensity (Stull, 2017).
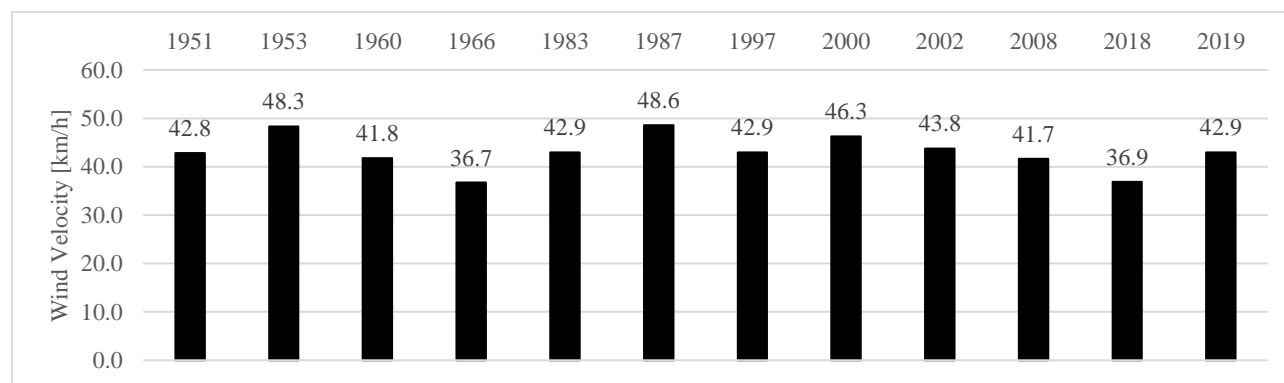
315 **Figure 7: Geostrophic velocity comparisons.**

The geostrophic wind velocity, calculated in correspondence of the central phase of the event (stage "D" in Figure 3), exhibit
a range comprised between 35 km/h – 50 km/h (Figure 7). The results show that the events characterized by higher velocities
have been also interested in more intense rainfall, such as the case of 1987, but on average the events have shown similar
values. Regarding the wind direction, not reported, it was observed that all the events have been characterized by the
320 presence of sustained southern flows at 850 hPa geopotential height. This evidence is in accordance with the typical air
masses configuration that characterizes this type of event where orographic precipitations are enhanced in intensity and they
are generally prolonged for several hours or days (Grazzini, 2007; Rotunno and Houze, 2007). The interpretation of
geostrophic balance of wind is generally valid at large scale but it does not take into account the secondary effects that can
modify consistently the local intensities of rainfall phenomena (Martin, 2006; Stull, 2017). Therefore, other terms of Eq. (4)
325 are further discussed.

3.2.2 Air Masses Evolution Paths

For determining the $T2$ term, ("boundary layer pumping" Equation (4.b)), the air masses evolution paths were examined during each event. Respect to the $T1$ and $T3$ terms, it acts inhibiting the ECs development and it is rather influenced by ECs latitude evolution. In fact, ECs do not follow the same advection path seasonally and this is a key parameter for

330   distinguishing and interpreting different types of rainfall events.
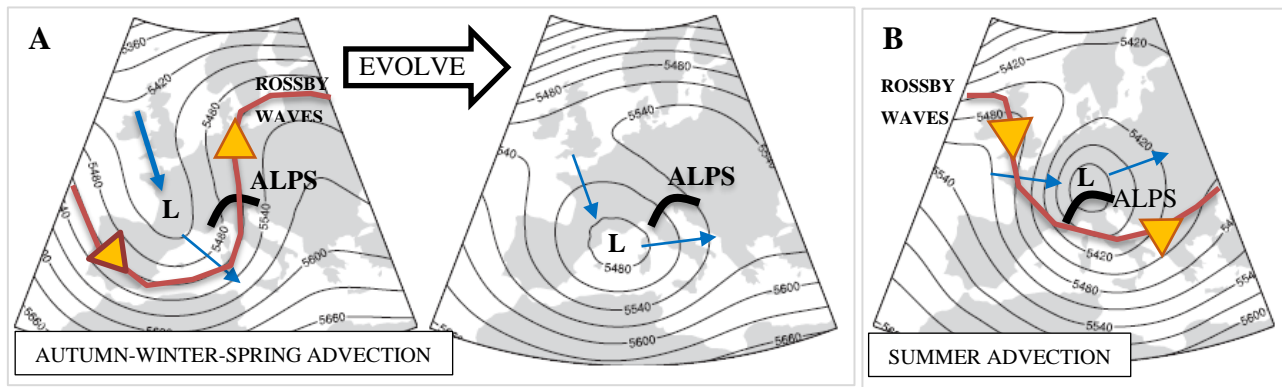
Figure 8: Extratropical Cyclone latitude extensions where are reported the most common air masses configurations for the autumnal and spring (A) and summer events (B), adapted from (Panziera, et al., 2015), modified after.

Looking at Figure 8.A the larger part of the autumnal events exhibits a meridian motion of the low pressure from the

335   northern part of Europe (Northern Sea) to the southern part, entering the Mediterranean Sea and moving eastward following Rossby waves track (Rotunno and Houze, 2007; Stull, 2017). This is the case of 1960, 1966, 2000, 2002 and 2018 events occurred between September and November. Autumnal periods are also characterized by the presence of high-temperature gradient between the Mediterranean Sea (warm) and the North Atlantic region (cold) which leads to the formation of strong EC structures more frequently (Rotunno and Houze, 2007; Stull, 2017).

340   Summer events of 1951, 1953, 1987, 1997 and 2019 exhibit a low-pressure tracking path that did not cross the Alps mountain range (Figure 8.B). This fact can be explained by considering that Rossby waves are in general northern shifted and less meandered during the summer period (Grazzini and Vitart, 2015; Martin, 2006). This reflects on the events that affect the southern side of the alpine region which are more rapid, less persistent, locally intense but not well organized such as the typical autumnal EC. In this framework, 1987 has assumed a character of exceptionality due to its anomaly features

345   regarding, in particular, its temporal persistence on the examined area.

3.2.3 Sea-Level Pressure Tendency Index

The $T3$ term has not explicitly analysed because it is represented as a linear function of the daily rainfall rate RR, which was already considered in the precipitation analysis. In particular, it is an expression of the local effects of the ECs on the territory, i.e. the rainfall intensity, and it is intimately bound with the thermodynamic of the ECs structure (Martin, 2006),

350   acting positively for its development (Stull, 2017).

In the end, the analysis of the intermediate components of the EC model $T1, T2$ and $T3$ terms allowed defining the Sea-Level Pressure Tendency index (SLPT) of Eq. (4).
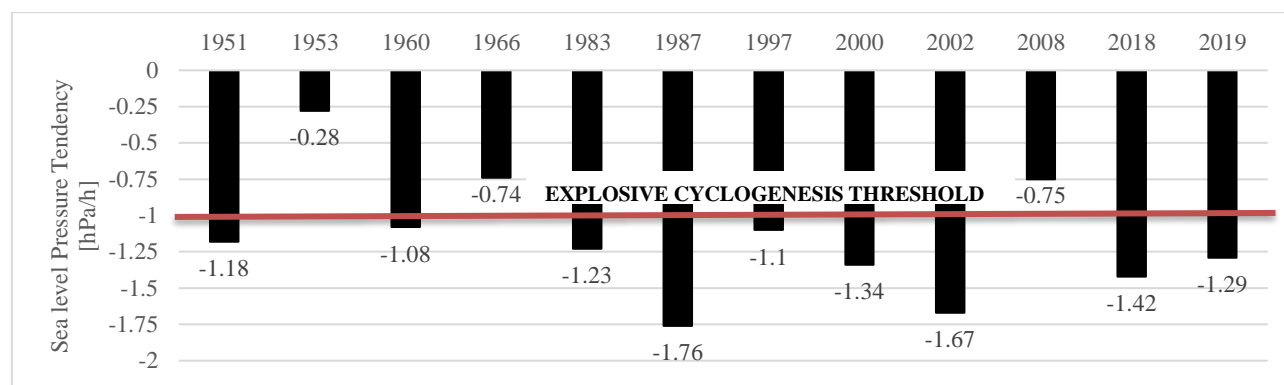
Figure 9: Sea-Level Pressure Tendency Index (SLPT) for the event analysed.

355 Looking at Figure 9, the SLPT index shows a range comprised between the – 0.28 hPa/h, recorded for the 1953 event and - 1.76 hPa/h recorded for 1987. The latter and the 2002 (-1.67 hPa/h) are reported to have been the EC structures with the highest intensity that affected the Northern Lombardy area. An important characteristic is that some of these ECs have been characterized by explosive cyclogenesis. Explosive cyclogenesis happens when an extratropical cyclone exhibits in its central part a low pressure deepening of 24 hPa in 24 h, which corresponds to an average rate of 1 hPa/h (Sanders and

360 Gyakum, 1980). They are potentially dangerous for the territory due to their rapid evolution, causing flash floods and diffuse hydrogeological issues that, in our case, have been confirmed by the historical chronicles found in the AVI and IFFI databases.

3.3 Magnitude Indexes Comparison

The SLPT index has been able to assess through a physical formulation the intensity of the meteorological triggering factors

365 of the hydrogeological event examined. Considering the rather strong cause-effect relation that was highlighted by historical chronicle among the intensity of the rainfall episodes and the severity of the subsequent hydrogeological issues, the SLPT index was tested as a predictor of the hazard magnitude. In order to address this, the index was normalized among 0 and 1 and then compared with the empirical index (AVG index) proposed within rainfall analysis, that represent in our study the reference for magnitude evaluation.

370 Looking at Figure 10 it is rather clear how the two indexes, the empirical and the physical based, are in accordance, giving a similar magnitude ranking of the events studied. In particular, both have addressed again the 1987 and 2002 as the two most critical of the entire dataset and have ranked 1953 as the lowest intense. For the other events, the ranking was rather similar showing an overall root mean square error (RMSE) less than 7%.
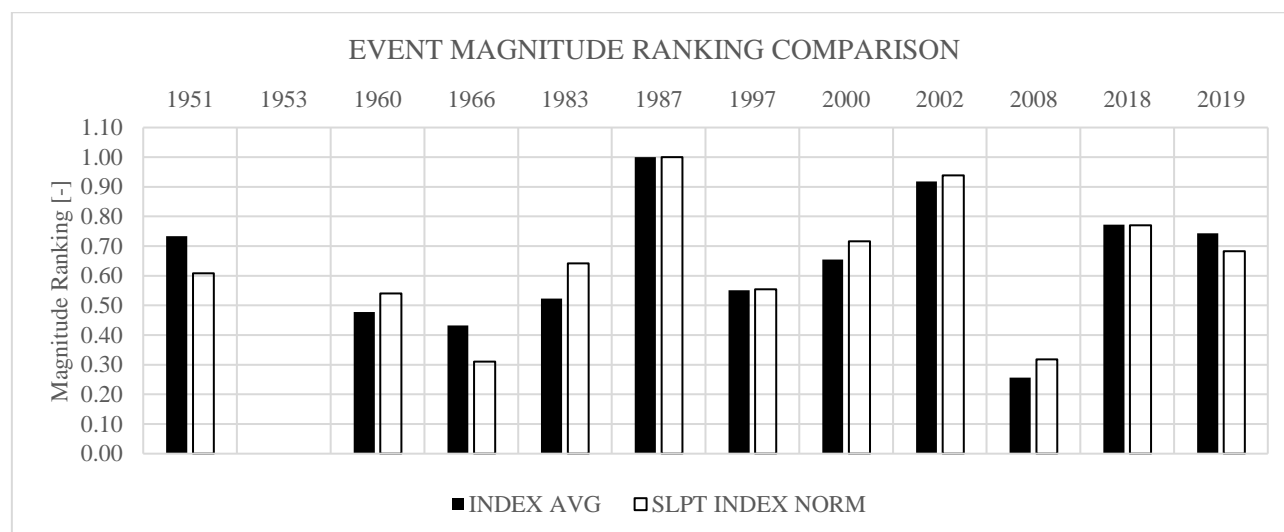
Figure 10: Event magnitude comparison between the SLPT index and the AVG index. The two indexes are normalized among 0 and 1.

The result obtained here are representative of the qualitative information found inside the historical database analysed, where an objective criterion for the magnitude quantification was not applicable due to poorly data reported (ISPRA, 2018). In this light, NCEP reanalysis map have represented an important source for the quantitative interpretation of the meteorological triggering factors in correspondence of the critical events analysed, allowing also a more complete examination of the severity of the subsequent rainfall induced hydrogeological events.

4 Conclusions

This study presented an extended back analysis of the triggering meteorological factors that have caused in the past several hydrogeological issues in the alpine mountain territory of the Sondrio Province, Northern Lombardy, Italy.

Excluding the analysis of the local geomorphological predisposing causes, the attention was pointed out on the characteristics of rainfall that were considered as the primary cause of hydrogeological hazards analysed. The main goal of the study was to develop a quantitative analysis of the meteorological triggering factors that were able to explain the magnitude of the rainfall induced hydrogeological issues that affected the studied area. Two different approaches have been proposed: the first one considered the local information about rainfall amounts, intensities, and durations for characterizing the critical events through the rainfall threshold curves. The second takes into account other meteorological parameters implicated in the physical description of a rainfall phenomenon.

Following the first approach, the rainfall threshold curves have been able to predict the instabilities, but no useful information was gathered for the magnitude assessment of the hydrogeological events. The analysis was improved considering the return period of precipitation. Nevertheless, looking only at the RPs may lead to a misleading and wrong

395   interpretation of the triggering causes because recorded rain-gauges data series represent a local estimation of the rainfall event intensity. The RP values do not take into account explicitly the spatial distribution of the meteorological phenomena that are directly correlated to the consequent hydrogeological issues triggered in the territory. Therefore, a composite magnitude index for assessing a ranking of hydrogeological events considered has been proposed taking into account not only the intensity of the triggers, i.e. return period of rainfalls, established from the analysis of the rainfall series, but also the

400   information about the spatial extension of the affected areas.

In the second approach, a meteorological analysis of the triggering has been carried out taking into account the NCEP reanalysis maps. The model in Eq. (4) was implemented for the description of each meteorological event intensities through the physically based index SLPT. This index was chosen because considers not only the local rain-gauges series but also other meteorological variables that are descriptive of the whole dynamic of the triggering event. That physical index was

405   then normalized and compared with the previous empirical one obtained from the analysis of precipitation data.

Both two indices have shown good accordance in the assessment of the magnitude of the studied events. In particular, the 1987 and the 2002 events have been correctly ranked as the strongest of the entire dataset, caused by explosive cyclogenesis. Respect to the m_1 and m_2 indices that are based on empirical evidence extracted from local data analysis, the SLPT indicator is physically based and can discriminate straightforwardly localized events "EXL" with respect to the more diffused ones

410   "DIF", that is a key information. The hydrogeological issues that affected the alpine territory were proportional to the overall intensity of extratropical cyclone systems and the SLPT index has been able to highlight this fact, also distinguishing the nature of the triggers.

In the view of the future climate change that, with high confidence (Faggian, 2015), will affect the Mediterranean and the Alpine environment, extreme meteorological events are supposed to increase (Ciervo et al., 2017; Gariano and Guzzetti,

415   2016; Moreiras et al., 2018). Our study moves in this direction, trying to consider integration between the traditional approach (i.e. local rainfall analysis) and the new instruments that meteorological models are starting to provide (i.e. meteorological reanalysis map) in order to give a comprehensive interpretation of the triggering factors of severe hydrogeological events.

420   *Code and data availability:* All the data reported in this paper are freely consultable on the Internet websites. In particular, reanalysis weather maps are freely downloadable from Meteociel Website (MeteoCiel, 2020), IFFI and AVI database are freely consultable and downloadable from (CNR, 2020; ISPRA, 2014), and Rain Gauges data are extracted from local Environmental Agency (ARPA Lombardia, 2020). The model applied in this work is also freely consultable and downloadable from (Stull, 2017).

425

Author Contribution: Andrea Abbate carried out the formal analysis and prepared the manuscript with contributions from all co-authors. Monica Papini supervised the research and Laura Longoni the review & editing.

430   *Competing Interests:* The authors declare that they have no conflict of interest.

References

Abbate, A., Longoni, L., Ivanov, V. I. and Papini, M.: Wildfire impacts on slope stability triggering in mountain areas, MDPI Geosciences, 9(417), 1–15, doi:https://doi.org/10.3390/geosciences9100417, 2019.

435   Albano, R., Mancusi, L. and Abbate, A.: Improving flood rick analysis for effectively supporting the implementation of flood risk management plans: The case study of "Serio" Valley, Envirnomental Science & Policy, 75, 158–172, doi:https://doi.org/10.1016/j.envsci.2017.05.017, 2017.

Andrews, D. G.: An Introduction to Atmospheric Physics, Cambridge Press, Cambridge., 2010.

ARPA Lombardia: Rete Monitoraggio Idro-nivo-meteorologico, [online] Available from:
440   www.arpalombardia.it/stiti/arpalombardia/meteo, 2020.

Ballio, F., Brambilla, D., Giorgetti, E., Longoni, L., Papini, M. and Radice, A.: Evaluation of sediment yield from valley slope, Transactions on Engineering Sciences, 67, 149–160, doi:http://doi.org/10.2495/DEB100131, 2010.

Bovolo, C. I. and Bathurst, J. C.: Modelling catchment-scale shallow landslide occurrence and sediment yield as a function of rainfall return period, Hydrological Processes, 26, 579–596, doi:https://doi.org/10.1002/hyp.8158, 2011.

445   Caine, N.: The rainfall intensity duration control of shallow landslide and debris flow, Geografisika Annaler, 62(1–2), 659–675, doi:https//doi.org/10.2307/520449, 1980.

Ceriani, M., Lauzi, S. and Padovan, M.: Rainfall thresholds triggering debris-flow in the alpine area of Lombardia Region, central Alps – Italy, in In Proceedings of the Man and Mountain'94, Ponte di Legno (BS), Italy., 1994.

Ciccarese, G., Mulas, M., Alberoni, P., Truffelli, G. and Corsini, A.: Debris flows rainfall thresholds in the Apennines of
450   Emilia-Romagna (Italy) derived by the analysis of recent severe rainstorms events and regional meteorological data, Geomorphology, 358, 1–20, doi:https://doi.org/10.1016/j.geomorph.2020.107097, 2020.

Ciervo, F., Rianna, G., Mercogliano, P. and Papa, M. N.: Effects of climate change on shallow landslides in a small coastal catchment in southern Italy, Landslide, 14, 1043–1055, doi:https://doi.org/10.1007/s10346-016-0743-1, 2017.

CNR: Sistema Informativo sulle Catastrofi idrogeologiche, [online] Available from: www.db.gndci.cnr.it, 2020.

455   COPERNICUS: Monitoring European climate using surface observations, [online] Available from: http://surfobs.climate.copernicus.eu/surfobs.php, 2020.

Corominas, J., van Westen, C., Frattini, P., Cascini, L., Malet, J.-P., Fotopoulou, S., Catani, F., Van Den Eeckhaut, M., Mavrouli, O., Agliardi, F., Pitilakis, K., Winter, M. G., Pastor, M., Ferlisi, S., Tofani, V., Hervás, J. and Smith, J. T.: Recommendations for the quantitative analysis of landslide risk, Bulletin of Engineering Geology and the Environment,
460   73(2), 209–263, doi:10.1007/s10064-013-0538-8, 2014.

De Michele, C., Rosso, R. and Rulli, M. C.: Il Regime delle Precipitazioni Intense sul Territorio della Lombardia: Modello di Previsione Statistica delle Precipitazioni di Forte Intensità e Breve Durata, ARPA Lombardia, Milano., 2005.

Faggian, P.: Climate change projection for Mediterranean Region with focus over Alpine region and Italy, JESE, 4, 482–500, doi:https://dori.org/10.17265/2162-5263/2015.09.004, 2015.

465 Frattini, P., Crosta, G. and Sosio, R.: Approaches for defining thresholds and return periods for rainfall-triggered shallow landslides, Hydrological Processes, 23(10), 1444–1460, doi:10.1002/hyp.7269, 2009.

Gao, L., Zhang, L. M. and Cheung, R. W. M.: Relationships between natural terrain landslide magnitudes and triggering rainfall based on a large landslide inventory in Hong Kong, Landslides, 15(4), 727–740, doi:10.1007/s10346-017-0904-x, 2018.

470 Gariano, S. L. and Guzzetti, F.: Landslides in a changing climate, Earth-Science Reviews, 162, 227–252, doi:10.1016/j.earscirev.2016.08.011, 2016.

Godson, W. L.: A new tendency equation and its application to the analysis of surface pressure changes, Journal of Meteorology, 5, 227–235, 1948.

Grazzini, F.: Predictability of a large-scale flow conducive to extreme precipitation over the western Alps, Meteorology and
475 Atmospheric Physics, 95(3), 123–138, doi:10.1007/s00703-006-0205-8, 2007.

Grazzini, F. and Vitart, F.: Atmospheric predictability and Rossby wave packets, Quarterly Journal of the Royal Meteorological Society, 141(692), 2793–2802, doi:10.1002/qj.2564, 2015.

Guzzetti, F., Peruccacci, S., Rossi, M. and Stark, C. P.: Rainfall thresholds for the initiation of landslides in central and southern Europe, Meteorology and Atmospheric Physics, 98(3), 239–267, doi:10.1007/s00703-007-0262-7, 2007.

480 Iida, T.: Theoretical research on the relationship between return period of rainfall and shallow landslides, Hydrological Processes, 18(4), 739–756, doi:10.1002/hyp.1264, 2004.

ISPRA: Inventario Fenomeni Franosi, [online] Available from: http://www.isprambiente.gov.it/it/progetti/suolo-e-territorio-1/iffi-inventario-dei-fenomeni-franosi-in-italia, 2014.

ISPRA: Dissesto idrogeologico in Italia: pericolosità e indicatori di rischio, ISPRA, Ispra., 2018.

485 ISPRA: SCIA: Sistema Nazionale per l'elaborazione e diffusione di dati climatici, [online] Available from: http://www.scia.isprambiente.it, 2019.

Iverson, R. M.: Landslide triggering by rain infiltration, Water Resources Research, 36(7), 1897–1910, doi:10.1029/2000WR900090, 2000.

Kalnay, E., Kanamitsu, M., Kistler, R., Collins, W., Deaven, D., Gandin, L., Iredell, M., Saha, S., White, G., Woollen, J.,
490 Zhu, Y., Chelliah, M., Ebisuzaki, W., Higgins, W., Janowiak, J., Mo, K. C., Ropelewski, C., Wang, J., Leetmaa, A., Reynolds, R., Jenne, R. and Joseph, D.: The NCEP/NCAR 40-Year Reanalysis Project, Bull. Amer. Meteor. Soc., 77(3), 437–472, doi:10.1175/1520-0477(1996)077<0437:TNYRP>2.0.CO;2, 1996.

Longoni, L., Papini, M., Arosio, D. and Zanzi, L.: On the definition of rainfall thresholds for diffuse landslides, Transactions on State of the Art in Science and Engineerin, 53(1), 27–41, doi:https://doi.org/10.2495/978-1-84564-650-9/03, 2011.

495 Longoni, L., Ivanov, V. I., Brambilla, D., Radice, A. and Papini, M.: Analysis of the temporal and spatial scales of soil erosion and transport in a Mountain Basin, Italian Journal of Engineering Geology and Environment, 16(2), 17–30, doi:https://doi.org/10.4408/IJEGE.2016-02.O-02, 2016.

Malamud, B. D., Turcotte, D. L., Guzzetti, F. and Reichenbach, P.: Landslide inventories and their statistical properties, Earth Surface Processes and Landforms, 29(6), 687–711, doi:10.1002/esp.1064, 2004.

500 Martin, J. E.: Mid-Latitude Atmosphere Dynamics, Wiley, Chichester, West Sussex, England., 2006.

MeteoCiel: Observations, Prévisions, Modèles en temps réel, [online] Available from: www.meteociel.fr, 2020.

Montrasio, L.: Stability of soil-slip, Wit Press, Risk Analysis II, 45, 357–366, doi:https://doi.org/10.2495/RISK000331, 2000.

Montrasio, L. and Valentino, R.: Modelling Rainfall-induced Shallow Landslides at Different Scales Using SLIP - Part II, 505 Procedia Engineering, 158, 482–486, doi:10.1016/j.proeng.2016.08.476, 2016.

Moreiras, S., Vergara Dal Pont, I. and Araneo, D.: Were merely storm-landslides driven by the 2015-2016 Niño in the Mendoza River valley?, Landslides, 15, doi:10.1007/s10346-018-0959-3, 2018.

NOAA: National Center for Environmental Information, [online] Available from: https://www.ncei.noaa.gov/, 2020.

Olivares, L., Damiano, E., Mercogliano, P., Picarelli, L., Netti, N., Schiano, P., Savastano, V., Cotroneo, F. and Manzi, M. 510 P.: A simulation chain for early prediction of rainfall-induced landslides, Landslides, 11(5), 765–777, doi:10.1007/s10346-013-0430-4, 2014.

Ozturk, U., Tarakegn, Y., Longoni, L., Brambilla, D., Papini, M. and Jensen, J.: A simplified early-warning system for imminent landslide prediction based on failure index fragility curves developed through numerical analysis, Geomatics, Natural Hazards and Risk, doi:10.1080/19475705.2015.1058863, 2015.

515 Papini, M., Ivanov, V., Brambilla, D., Arosio, D. and Longoni, L.: Monitoring bedload sediment transport in a pre-Alpine river: An experimental method, Rendiconti Online della Società Geologica Italiana, 43, 57–63, doi:10.3301/ROL.2017.35, 2017.

Peres, D. J., Cancelliere, A., Greco, R. and Bogaard, T. A.: Influence of uncertain identification of triggering rainfall on the assessment of landslide early warning thresholds, Natural Hazards and Earth System Sciences, 18(2), 633–646, 520 doi:10.5194/nhess-18-633-2018, 2018.

Piciullo, L., Gariano, S. L., Melillo, M., Brunetti, M. T., Peruccacci, S., Guzzetti, F. and Calvello, M.: Definition and performance of a threshold-based regional early warning model for rainfall-induced landslides, Landslides, 14(3), 995–1008, doi:10.1007/s10346-016-0750-2, 2017.

Rappelli, F.: Definizione delle soglie pluviometriche d'innesco frane superficiali e colate torrentizie: accorpamento per aree 525 omogenee, IRER, Istituto Regionale di Ricerca della Lombardia, Milano., 2008.

Reid, L. and Page, M. J.: Magnitude and frequency of landsliding in a large New Zealand catchment, Geomorphology, 49, 71–88, doi:10.1016/S0169-555X(02)00164-2, 2003.

Rosi, A., Peternel, T., Jemec-Auflič, M., Komac, M., Segoni, S. and Casagli, N.: Rainfall thresholds for rainfall-induced landslides in Slovenia, Landslides, 13(6), 1571–1577, doi:10.1007/s10346-016-0733-3, 2016.

530 Rossi, M., Guzzetti, F., Salvati, P., Donnini, M., Napolitano, E. and Bianchi, C.: A predictive model of societal landslide risk in Italy, Earth-Science Reviews, 196, 102849, doi:10.1016/j.earscirev.2019.04.021, 2019.

Rosso, R., Rulli, M. C. and Vannucchi, G.: A physically based model for the hydrologic control on shallow landsliding, Water Resour. Res, 42, doi:10.1029/2005WR004369, 2006.

535 Rotunno, R. and Houze, R.: Lessons on orographic precipitation for the Mesoscale Alpine Programme, Quarterly Journal of the Royal Meteorological Society, 133, 811–830, doi:10.1002/qj.67, 2007.

Sanders, F. and Gyakum, J. R.: Synoptic-Dynamic Climatology of the "Bomb," Mon. Wea. Rev., 108(10), 1589–1606, doi:10.1175/1520-0493(1980)108<1589:SDCOT>2.0.CO;2, 1980.

Stull, R. B.: Practical Meteorology: An Algebra-based Survey of Atmospheric Science., University of British Columbia, Vancouver, Canada., 2017.

540 Tropeano, D.: Inondazioni e frane in Lombardia: un problema storico, in Utilizzo dei dati storici per la determinazione delle aree esondabili nelle zone alpine, pp. 47–109, CNR-IRPI, Torino., 1997.

Wallace, J. M. and Hobbs, P. V.: Atmospheric Science: an introductory survey, Elsevier, Oxford., 2006.